Communications Earth & Environment https://doi.org/10.1038/s43247-026-03860-x

Article in Press

Canada's 2023 wildfire smoke caused a 2.8 percent drop in solar power generation, costing two billion dollars

Received: 24 March 2026

Accepted: 20 July 2026

Published online: 28 July 2026

Cite this article as: Roșu, I.-A., Jones, M.W., Grillakis, M. *et al.* Canada's 2023 wildfire smoke caused a 2.8 percent drop in solar power generation, costing two billion dollars. *Commun Earth Environ* (2026). https://doi.org/10.1038/s43247-026-03860-x

Iulian-Alin Roșu, Matthew W. Jones, Manolis Grillakis, Manolis P. Petrakis, Matthew Kasoar, Rafaila-Nikola Mourgela, Lampros Gkounelas & Apostolos Voulgarakis

Canada's 2023 wildfire smoke caused a 2.8 percent drop in solar power generation, costing two billion dollars

Iulian-Alin Roșu[1,2*], Matthew W. Jones[3], Manolis Grillakis[1,2], Manolis P. Petrakis[1,2], Matt Kasoar[2,4], Rafaila-Nikola Mourgela[1,2], Lampros Gkounelas[1] and Apostolos Voulgarakis[1,2,4]

1 School of Chemical and Environmental Engineering, Technical University of Crete, Chania, Greece (irosu@tuc.gr, egrillakis@tuc.gr, epetrakis1@tuc.gr, rmourgela@tuc.gr, lgkounelas@tuc.gr, avoulgarakis@tuc.gr)

2 Leverhulme Centre for Wildfires, Environment and Society, Imperial College London, London, UK (m.kasoar12@imperial.ac.uk)

3 Tyndall Centre for Climate Change Research, School of Environmental Sciences, University of East Anglia, Norwich Research Park, Norwich, UK (matthew.w.jones@uea.ac.uk)

4 Department of Physics, Imperial College London, London, UK

* Correspondence to: irosu@tuc.gr

Abstract

The record-breaking 2023 Canadian wildfires led to extreme emissions of aerosols, with plumes extending across the Northern Hemisphere. This study highlights the potential impact of such emissions on photovoltaic energy production across North America and Europe using a state-of-the-art Earth system model. Our results show substantial radiative and temperature anomalies during May–September 2023, with radiative impacts leading to a total 5-monthly modelled photovoltaic production deficit of -6.38 ± 8.86 terawatt hours (one standard deviation) across North America and Europe (2.8% of total 5-monthly photovoltaic generation). The carbon burden of this solar power production loss is estimated at 2.083 ± 2.656 megatons of carbon dioxide (one standard deviation), with a total economic deficit of 1.88 ± 2.71 billion US dollars (one standard deviation). Despite greater North America modelled photovoltaic losses, the associated monetary deficit is higher in Europe. These findings emphasize that resilience of photovoltaic production can be challenged by large-scale wildfire events, highlighting the need for integrated transnational and intercontinental strategies in climate mitigation, energy security, and wildfire prevention.

Introduction

Efforts to mitigate climate change require a rapid transition to renewable energy sources, among which solar energy plays a central role [1] [2]. To "ensure access to affordable, reliable, sustainable and modern energy for all", as seen in the 7th goal of the United Nation's sustainable development goals (United Nations, 2015: Sustainable Development Goals. https://sustainabledevelopment.un.org/sdgs), it is necessary to shift away from fossil-fuel based energy to renewable energy. Utility-scale photovoltaics (PV) are becoming increasingly viable given decreases in production costs by 82% from 2010 to 2020 [3], and in 2023 PV generation accounted for 5.5% (pv magazine USA. https://pv-magazine-usa.com/2024/02/29/solar-generated-5-5-of-u-s-electricity-in-2023-a-17-5-increase) and 9% (EUROSTAT. https://ec.europa.eu/eurostat/web/interactive-publications/energy-2025) of total generation in the USA and Europe, respectively.

However, energy suppliers and grid operators must account for any sources of lost irradiance when building risk and resilience into the energy systems. One such source of variability is high atmospheric aerosol loadings, which can attenuate a consequential fraction of the incoming solar irradiance [4] [5]. The influence of aerosols on attenuation strongly depends on their physical and chemical composition [6] [7] [8], and in some regions their impact on photovoltaic (PV) generation can rival that of clouds [9]. For example, reductions in PV power anywhere between 13% and 22% have been observed in West Africa due to high atmospheric aerosol loads [10]. Smoke from wildfires is an important factor driving high atmospheric aerosol loads and increased cloud cover worldwide [11] [12] [13] [14]. Higher temperatures, earlier snowmelt, and increased fuel aridity have extended wildfire seasons and caused more extreme wildfire events since the mid-1980s in North America (NA) [15] [16], and these conditions are projected to worsen as the climate continues to change. Historical [17] [18] and projected [19] air quality trends indicate that 21st century wildfire smoke emissions even offset declining anthropogenic PM emissions in parts of the Northern Hemisphere, including most of Canada and the NA Cordillera [20].

Wildfire smoke diminishes PV energy production by reducing the solar radiation that reaches installations, with important implications for grid planning and operations [21]. Numerous case studies report substantial reductions during wildfire events: a 34% drop in average output over two days at a PV plant in Spain [22], an average 7% reduction at a solar lab in Australia during a controlled burn with AOD of 0.25, peaking at 27% [23], and a 8.3% decline across 53 utility-scale PV plants in the western United States during the 2018 wildfire season [24] along with reductions of 10–50% in southern California during the 2020 season, with AOD values of 0.5–4.5 [25].

Studies evaluating the large-scale impacts of wildfire aerosols on solar power have been limited to the US and preceded the most significant wildfire smoke emissions event in NA history, related to extensive wildfires across Canada [24] [26]. Between May and September 2023, nearly 5% of Canada's forested area burned down (Canadian Interagency Forest Fire Centre. https://ciffc.ca/sites/default/files/2024-03/03.07.24_CIFFC_2023CanadaReport%20%281%29.pdf) (Canadian Minister of Natural Resources. https://natural-resources.canada.ca/forest-forestry/much-forest-does-canada-have), seven times the average annual area lost over the past 40 years [27]. This event produced the largest wildfire emissions ever recorded in Canada (Atmosphere Monitoring Service, Copernicus. https://atmosphere.copernicus.eu/copernicus-emissions-canadian-wildfires-highest-record-smoke-plume-reaches-europe), comparable to the annual fossil fuel emissions of large nations [28]. Large quantities of aerosols and gases were released, significantly impacting air quality and climate [28]. Notably, CO_2 emissions from this event exceeded those from all tropical tree cover loss in 2023 by 25% [29]. Although previous wildfire events have had widespread impacts [30] [31], the 2023 Canadian wildfires were unprecedented in scale [28]. A detailed spatial analysis is presented in [32].

In this work, we examine the modelled large-scale impact on PV production of the 2023 Canadian wildfire emissions, as an example of a particularly large wildfire with emissions that spread over large distances. Both direct and indirect atmospheric effects of these emissions were observed and modelled across the Northern Hemisphere in our previous work [33], including analysis and validation of the model data employed in this study, derived from the EC-Earth3 Earth System Model [34]. Ensembles were run with ("FIRE") and without ("noFIRE") the 2023 Canadian wildfire emissions, and in this research, we compare surface downwelling flux between these runs which enables direct inference of modelled reductions in solar power output. This data has been extracted from the Copernicus Atmosphere Monitoring Service (CAMS) Global Fire Assimilation System (GFAS) [35].

Results

Lost solar power generation due to wildfire smoke transport

Model data shows that smoke from the Canadian wildfires drove a -6.38 ± 8.86 TWh (one standard deviation) reduction in solar power generation across Canada, the USA, and Europe during 2023, equivalent to the annual energy demand of Luxembourg (Ember. https://ember-energy.org/data/yearly-electricity-data/) or of large cities such as Copenhagen, Denver, or Vancouver. It is also equivalent to 89.4% of the daily electric energy production of all nuclear power plants on the planet in 2023 (World Nuclear Association. https://world-nuclear.org/information-library/current-and-future-generation/nuclear-power-in-the-world-today). Of the three political entities, despite overall higher energy losses in Noth America, Europe also experienced, on average, significant loss of solar power production (3.02 TWh), with Germany experiencing a 1.19 TWh reduction in solar power generation alone. Figure 1 shows the state and country level variation in lost PV generation, with the Canadian province of Ontario and US state of California showing the greatest loss of production for their respective countries (Fig. 1).

We explicitly account for the cooling effect of aerosols on PV efficiency in our calculations (see Methods). The direct radiative effect from aerosol presence on energy production is -3.64 TWh, -3.38 TWh, and -0.5 TWh while the corresponding temperature effect on energy production is 0.62 TWh, 0.47 TWh, and 0.04 TWh for Europe, USA and Canada respectively. Therefore, the cooling effect compensates the radiative effects by the following percentages: 20.5% in Europe, 16.3% in the USA and 8.4% in Canada. This percentage rises in increasingly distant areas because the temperature effect of aerosols extends over a larger distance than the radiative effect, as the radiative effect mostly depends directly on aerosol presence and induced cloud cover modifications whereas the temperature effect also propagates through advection from the regions of greatest temperature anomaly to regions that are much further away. A discussion of the minor radiative influence of the "soiling" (deposition of aerosols) of PV installations has been added to the supplementary material.

The NA region and the European region have relatively similar PV production setbacks (slightly higher in the NA case) even though the NA region is much more affected by the wildfire emissions. This is explained by the fact that, despite Europe undergoing a less intense radiative effect, it contains a more developed and productive PV infrastructure when compared to the NA region. A plot of the extent of the modelled surface downwelling shortwave flux due to wildfire smoke transport is shown in the Methods section.

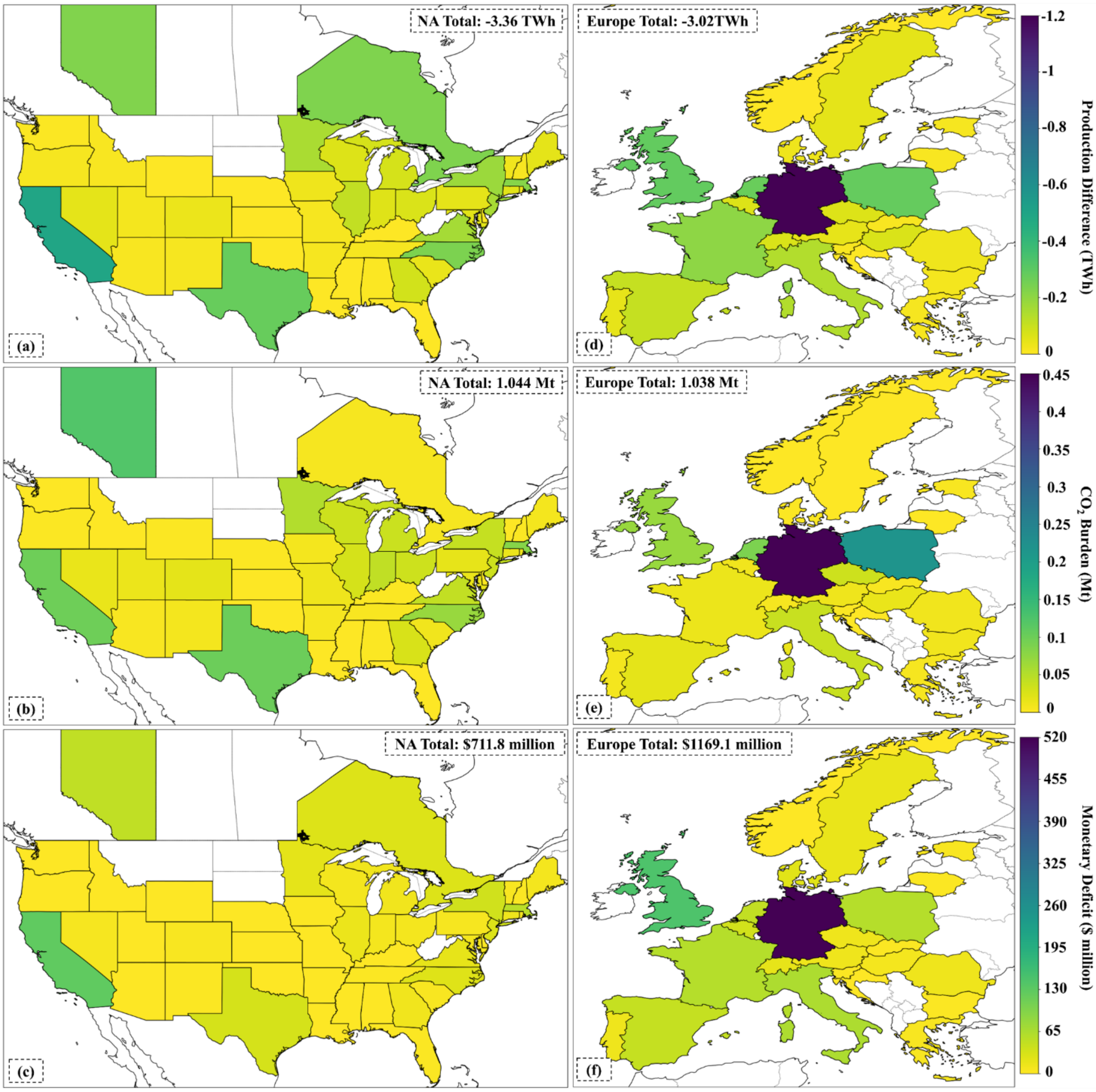

Carbon footprint of the lost solar power generation

Due to the loss of PV generation from the modelled radiative effect of the 2023 Canadian wildfires, other sources of energy were required to fulfil continued demand for energy, which produced a significant carbon footprint. The consequent CO_2 emissions from the USA, Canada and Europe given our modelled irradiance impacts was 2.083 ± 2.656 Mt CO_2 (one standard deviation) (Fig. 1). The CO_2 burden is only slightly higher in the NA region. Both the European and NA energy infrastructures seem to have very similar robustness to PV deficits on average given the fact that the CO_2 burden is almost the same.

According to the greenhouse gas equivalencies calculator provided by the United States Environmental Protection Agency (EPA, https://www.epa.gov/energy/greenhouse-gas-equivalencies-calculator), the total CO_2 burden is equivalent to approximately 496,000 gasoline-powered passenger vehicles driven for one year, approximately 280,000 typical USA homes energy use for one year, and it is equivalent to carbon sequestered by roughly 2 million acres of USA forests in one year (0.25% of all forested land in the USA). Comparing this total CO_2 burden with natural events, it is equivalent to 14% of the annual CO_2 output from Mount Etna [36], and to 10% of the CO_2 emitted by European wildfires in 2023 (Reuters. https://www.reuters.com/world/europe/europes-wildfires-2023-were-among-worst-this-century-report-says-2024-04-10/).

Financial impact of power grid responses to lost solar power generation

We estimated the economic implications of lost PV generation based on a market-based approach supplemented by an assessment of the social cost of carbon incurred through heightened use of fossil fuel-based energy generation (see Methods). The modelled total monetary deficit across all countries and states contained in this analysis is \$1.88 ± 2.71 billion (one standard deviation). This figure is significant, given that in 2023 wildfires had an estimated impact of 4.1 billion euros in Europe in terms of average economic cost per hectare burned ("Greece Suffers Most Damage as Wildfires Cost Europe €4.1 Billion." Bloomberg. https://www.bloomberg.com/news/articles/2023-09-04/greece-suffers-most-damage-as-wildfires-cost-europe-4-1-billion), not accounting for the European modelled deficit calculated in this study. The global solar PV panel market value has been estimated at \$170.25 billion euros in 2023 (Grand View Research. https://www.grandviewresearch.com/industry-analysis/solar-panels-market), meaning that the estimated inflicted cost by the 2023 Canadian wildfire aerosols was equal to 1.1% of the total global solar PV panel market. The monetary deficit in the NA region is lower than the European deficit. This difference results from the market value of electricity being generally smaller in the USA.

A final consideration regarding the financial aspect of this research is that electric power trade flows can also be considered, but because we have employed mostly 2022 data for the PV production of each country or state, 2022 trading data would reflect a scenario unaffected by the emissions. At best, it is possible to qualitatively gauge if there is any correlation between the 5-monthly interval and electric power trading modification in 2023 in the most affected country, which is Germany. An investigation of German electricity imports reveals a historical 5.8 TWh import in August 2023, highest in the entire dataset (2015-2025), along with similar if slightly less significant values in the rest of the 5-monthly period (SMARD (Strommarktdaten), Bundesnetzagentur, Germany. https://www.smard.de/en/). Even though this import is far higher than the modelled 5-monthly production difference for Germany, and it has mostly resulted from Germany's transition to a low-carbon and nuclear-free economy (Clean Energy Wire.

https://www.cleanenergywire.org/germanys-energiewende-brief), one could argue that the production difference caused by the wildfire emissions exacerbated a vulnerable energy transition period with an energy deficit.

Discussion

Our model results show that severe wildfire emissions can damage the renewable energy sector. Additionally, smoke from wildfires is linked to severe public-health impacts and billions of dollars in healthcare costs [37] [38] [39] [40], reinforcing the broader monetary consequences. In determining why some areas are modelled to have suffered a greater impact than others, the radiation impact ΔR is not sufficient, and marginal emission factors (EF_m) along with seasonal ratio (SR) values must also be considered. To quantify this consideration, it is possible to graphically represent whether a given EF_m and SR of a given country or state are higher than their respective regional averages (Fig. 2). In this case, Canada is not considered because there are only two relevant provinces in our analysis.

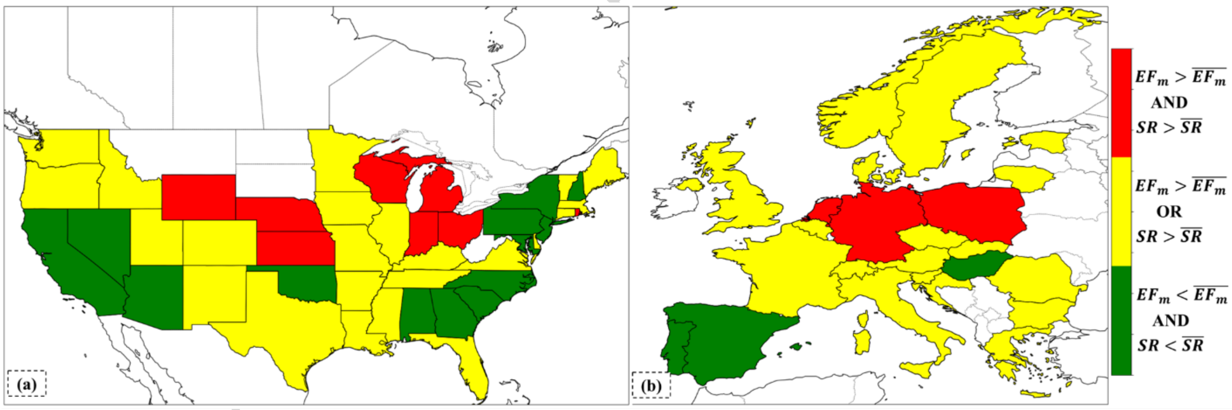

Since a country's EF_m is high when its electricity grid is more reliant on carbon-intensive power sources, and since the SR, while dependent on geographical factors, can be ameliorated through various technical PV particularities (which shall be discussed shortly), the two cases could be described as: in the case of $EF_m > \overline{EF_m}$ their energy production infrastructure did not implement sufficient "green" contingencies, and in the case of $SR > \overline{SR}$ their geographic or meteorological parameters led to unfavourable seasonality for PV production and/or improvements could have been made to the efficiencies of the PV infrastructures.

As per Fig. 2, in the USA region, the states coloured in red are northern and central states which are also among the most affected by the aerosol impacts, and they are states which do not have large $P_{5-monthly}$. Meanwhile, the states with the highest $P_{5-monthly}$, which are California, Texas, North Carolina, Nevada and Arizona, experience the least radiative effects from the emissions in the USA (even though California shows the highest energy loss) and are also states presenting a favourable case analysis (Fig. 2). In contrast, the European countries with the highest

$P_{5-monthly}$, which are Germany, France, Spain, Italy and the Netherlands exhibit a more unfavourable case analysis, and the countries presenting the most unfavourable case (Germany, Netherlands and Poland) were quite affected by the emissions comparatively to the rest of the European region. For these three countries, one can also investigate a trend: SR shifts from 2022 to 2024 show an increase of 3.78% for Germany, 4.58% for the Netherlands and 2.43% for Poland (ENTSO-E – European Network of Transmission System Operators for Electricity. https://www.entsoe.eu/data/power-stats/). Official EF_m for Europe cannot be found later than 2021 (European Commission, Joint Research Centre (JRC). https://publications.jrc.ec.europa.eu/repository/handle/JRC136340), but for a qualitative analysis one can use Nowtricity (Nowtricity. https://www.nowtricity.com/) to find decreases of 18.38% for Germany, 30% for the Netherlands and 2.3% for Poland. For the countries with the most unfavourable case analyses, there is a recent slight increase in seasonal ratio but a substantial decrease in emission factors with one exception, which indicates a short-term increase in energy production resilience to radiation blocking events for Germany and the Netherlands, if trends continue. Conversely, the data indicates a worrying short-term stagnation in energy production resilience to radiation blocking events in the case of Poland.

For such future wildfire impacts to be diminished, the countries and states contained in this analysis can implement measures and policies to decrease EF_m and to mitigate SR. Improving the conditions of countries or states in condition $EF_m > \overline{EF_m}$ can be done by diversifying renewable portfolios and modifying "non-green" sources so that they are less polluting. In the case of $SR > \overline{SR}$, the seasonality of a country largely depends on its geographical position, however certain methods can improve PV performance in less-than-ideal seasonal conditions. For example, replacing direct PV systems which are inefficient under diffuse light, or using passive cooling techniques and "floatovoltaics" [41], or using PV installations with higher DC/AC ratios [42] and using microinverters which increase system performance under diffuse lighting conditions and partial shading [43] [44]. While PV power remains one of the most simple and reliable sources of green electricity, and this is accentuated both by forecasted increases in mean total radiation [45] and by stabilization of solar resource seasonality [46], wildfire trends are also characterised by extended seasons, longer burns and larger burned areas [15] [16]. In these conditions and given the findings of this study, the entire NH might suffer general temporary decreases in PV output for such extreme wildfire events. Thus, it can be argued that countries throughout the NH should increase transnational cooperation to work towards preventing such events for the interest of all, as extreme wildfires are seen to affect not just public safety and ecology but also PV energy production.

To conclude, the impacts of the 2023 Canadian wildfire event are a critical example of how large-scale biomass burning can change the atmospheric radiative balance and affect renewable energy production far beyond emission source regions. Using a state-of-the-art Earth system model, this study demonstrates that wildfire-induced aerosol loading led to significant modelled declines in PV energy generation across NA and Europe. The analysis also shows that the modelled surface cooling induced by wildfire aerosols was insufficient in offsetting the overall energy deficit. These results highlight that large wildfires can have trans-boundary implications for solar energy production, compounding the economic and environmental costs of climate change, and that PV energy planning and resilience strategies should account for wildfire aerosol variability.

Methods

Model configuration

This study has used the EC-Earth3 Earth system model in its standard EC-Earth3-AerChem configuration, incorporating an atmospheric component ("Integrated Forecasting System cycle 36r4", IFS 36r4), an ocean component ("Nucleus for European Modelling of the Ocean 3.6", NEMO 3.6), and an atmospheric chemistry component ("Tracer Model 5", TM5) [34] [47]. Within the AerChem scheme, which has its atmospheric chemistry component coupled with an aerosol microphysics scheme, a comprehensive set of tropospheric aerosol species (core species are sulfate, black carbon, primary and secondary organic aerosols, sea salt and mineral dust) and aerosol – chemistry interactions are covered [47]. The aerosol species are simulated using the M7 modal aerosol microphysics scheme, which contains 4 soluble modes (nucleation, Aitken, accumulation, coarse) and 3 insoluble modes (Aitken, accumulation, coarse), predicting both particle number and mass for each mode and including new particle formation, condensation, aging, hygroscopic growth, sedimentation and deposition [47]. The model is run in a fully coupled atmosphere-ocean configuration to allow the model meteorology to respond freely to the simulated effects of the wildfire emissions, and we use an ensemble of free-running simulations with small variations in initial atmosphere and ocean states.

Two sets of model experiments over the period from May to December 2023 were conducted, with ten ensemble members each. The first set included the 2023 Canadian wildfire emissions as input ("FIRE"), while the second excluded them ("noFIRE"). The results presented in this work are derived from the means of these ensembles. To introduce variability, individual ensemble members were initialized from consecutive start dates, with the first member beginning on January 1st, the second on January 2nd, and so forth. The uncertainty calculation for the main results in this paper is expressed as one standard deviation of intermember variability. Significance stippling (seen in Fig. 3) represents the application of Student's t-tests for statistical significance via the SciPy library in Python, and our code was developed in Python 3.12. For the initialization of the simulation, we used atmospheric and ocean variables for year 2015, due to model data availability restrictions. The fact that we are using initial conditions from a different year to the emissions is expected to have little impact, given the objective of this study which is to establish the potential large-scale effects of emissions of the magnitude of those that occurred in Canada in 2023 in general, rather than to specifically model the exact atmospheric conditions of 2023. Data used as wildfire emissions input has been extracted from the Copernicus Atmosphere Monitoring Service (CAMS) Global Fire Assimilation System (GFAS) [35].

In our results, the ensemble spread exceeds the ensemble-mean response, reflecting the large intrinsic variability of aerosol–cloud–radiation interactions. Similar standard deviation characteristics have been reported in previous studies of fire aerosol radiative forcing and broader aerosol forcing uncertainty, and fire aerosol radiative short-term effects are difficult to isolate because the atmospheric response contains substantial internally generated variability [48] [49] [50]. Regarding the modelled vertical transport of wildfire aerosols, past research has shown that atmospheric chemistry models such as TM5 underestimate BBA plume altitudes when compared to CALIOP data [51]. It is currently theorized that the bias is due to wet deposition being too strong in this model [52]. However, this is expected to have a low impact in terms of aerosol radiative effects, as under cloudless skies changing the altitude of an artificial aerosol layer has a minor impact on the levels of shortwave radiation at the top and bottom of the atmosphere, even for high aerosol loads [53]. Furthermore, wildfire aerosols fall in the category of least sensitive to altitude in terms of the relation between their radiative effects and layer height [54]. TM5 can also present errors in modelled aerosol lifetime, however, with regards to the CALIOP data comparison TM5 presents a median performance relative to the rest of the models [51].

Modelled anomalies and temperature considerations

In general, PV power output is can be approximated as linearly proportional to incident solar irradiance [26] [55] [56]. In particular, it has been previously shown that the operational segments of I-V curves in both modelled and measured PV installations present linear proportionality between current and irradiation [56]. Ambient temperature is another relevant environmental factor [56], since lower temperatures can slightly increase PV efficiency, meaning that the cooling effect (direct and indirect) of aerosols may partly offset radiation-driven losses. Nonetheless, experimental and modelled I–V curves in [56] clearly show that incident radiation is the dominant driver, with temperature fluctuations playing a secondary role, thus we temporarily assume that the percentage reduction in downward radiation due to aerosol effects translates directly into proportional PV power losses, with any gains from surface cooling treated as correction which will be elaborated later in this study. Specifically, we focus on the percentage difference in surface downwelling flux between the FIRE and noFIRE model runs. This percentage is obtained as:

$$\Delta R = 100\,\frac{R_{FIRE}-R_{noFIRE}}{R_{noFIRE}} \qquad (1)$$

wherein R_{FIRE} is the surface downwelling shortwave flux in the FIRE runs and R_{noFIRE} is the surface downwelling shortwave flux in the noFIRE runs, and the figure below (5-monthly, May-September 2023 model output average) is the result. The percentage is plotted below, along with the surface temperature difference between the FIRE runs and noFIRE runs, caused by climate system responses to the decrease in surface downwelling shortwave flux.

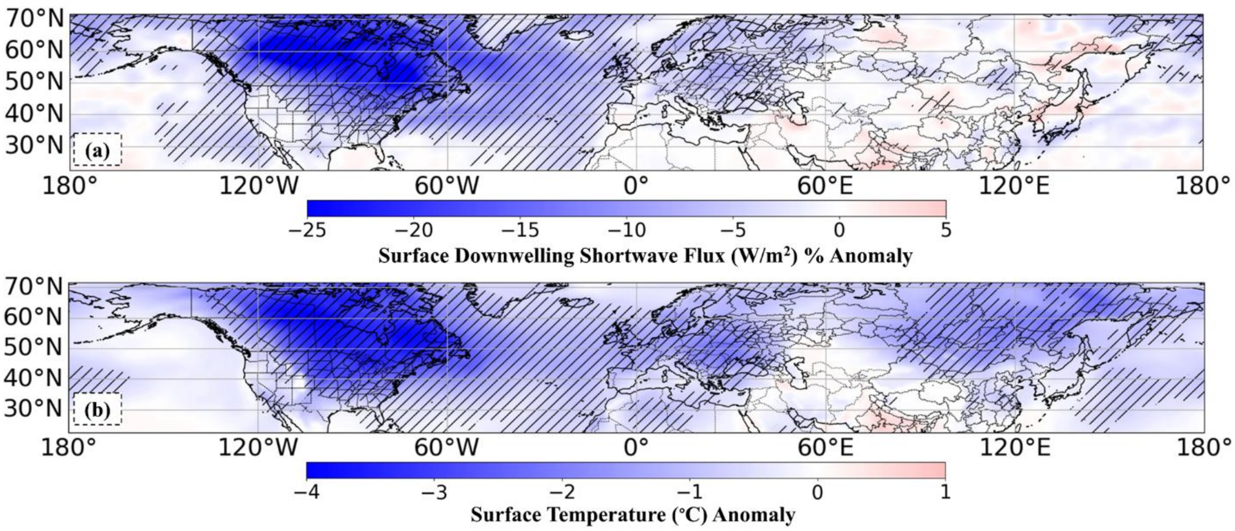

A country-wise and state-wise approach is taken to quantify the impacts of the emissions in more detail. Canada, the USA, and Europe were the principally affected regions in terms of surface downwelling shortwave flux (Fig. 3). Of the three regions, some states and countries were excluded from our state- and country-level analysis because they either produce less than 0.1 TWh of PV production per year, lack reliable official data on PV production, capacity, or carbon footprints, or are affected by geopolitical issues. Areas that were also excluded are North Africa and NH Asia. In the case of North Africa, the 5-monthly radiative effect is negligible, and regarding the rest of NH Asia, the 5-monthly radiative effect is not coherent enough making it difficult to determine which of the effects are due to the aerosols and which are model-inherent noise. It should also be noted that, given the fact that some countries or states (Spain and California, for instance) lack full coverage of statistically significant impacts, it is possible that the total results presented in our work could be lower than reported.

Increases in electric power production due to surface cooling can also be investigated. A previous study found that, for Greece, climate change effects on PV production result from opposing factors: higher mean total radiation increasing output, and higher surface temperatures reducing it. [45]. That study found the modelled $5W/m^2$ increase in radiation outweighs the up to 3.5°C increase in surface temperature, leading to an overall 4% increase in PV energy output. Taking this into account with our modelled values (with the minima being $-25W/m^2$ and -4°C), the cooling effect will be much lower than the radiative effect, however a clear relationship must be found which accounts for this cooling. Thermal inertia arguments can be safely ignored since our analysis deals with a multi-month average. A straightforward relation between PV cells efficiency and temperature along with solar irradiance can be obtained from the literature, with the temperature sensitivity to be roughly estimated to 0.54%/°C [57] [58]. We arrive at a relation which solely connects PV efficiency with temperature:

$$\frac{\eta}{\eta_{ref}} = 1 - 0.0054\Delta T \tag{2}$$

wherein $\frac{\eta}{\eta_{ref}}$ is the efficiency ratio, 0.0054 is the average of the temperature coefficients for cell efficiency (β) reported in [59], and ΔT is the surface temperature difference between the FIRE runs and noFIRE runs. Given this relation, the 5-monthly modelled production difference accounting for both radiative effects and temperature effects is as follows:

$$\Delta P_{5-monthly}^{total} = \Delta P_{5-monthly}(1 - 0.0054\Delta T) \tag{3}$$

wherein $\Delta P_{5-monthly}$ has been defined as the modelled production difference due to aerosols accounting solely for radiative effects.

Solar power production data sources and processing

The following is a detailed account of the solar power data sources and data processing methods that have been employed in this study to account for solar power data scarcity and to calculate the implied modelled carbon footprint along with the monetary deficit resultant from the emissions of the wildfire event. Given the assumption that the reduction in generated power is approximately linearly proportional to the reduction of radiation, an estimation of how much solar power by country would have been generated had the aerosols not existed first requires us to know the yearly solar power generation of each analysed country and state. A reasonable starting point is yearly solar power generation inventories, however this data is not always reliable. The main issue is that some inventories do not properly consider domestic PV production. Official USA and Canadian inventories (US Energy Information Administration (EIA) Net Generation from Solar Photovoltaic. https://www.eia.gov/electricity/annual/html/epa_03_21.html), and the IEA Photovoltaic Power System Programme (IEA-PVPS) with Canadian Renewable Energy Association (CanREA) (Natural Resources Canada & Canadian Renewable Energy Association (CanREA). https://iea-pvps.org/wp-content/uploads/2023/11/National-Survey-Report-of-PV-Power-Applications-in-Canada-2022.pdf) do include domestic PV production through various means. The EIA collects data through various surveys and even reports PV modules shipment (EIA-63B) while publishing data which can also be broken down by sector, and the IEA-PVPS & CanREA report does consider domestic solar production directly and through projects such as Ontario's microFIT.

This situation does not extend to the whole of Europe since ENTSO-E (ENTSO-E – European Network of Transmission System Operators for Electricity. https://www.entsoe.eu/data/power-stats/) typically inventories the PV generation of merely European Union countries. There is also unreliability in ENTSO-E because of non-reporting of most domestic production for the UK, Netherlands and Switzerland, and therefore other sources must be used (Solar Power Portal (Informa PLC). https://www.solarpowerportal.co.uk/solar-pv/solar-pv-generation-increased-by-10-in-2022-says-desnz) (Statistics Netherlands (CBS). https://www.cbs.nl/en-gb/news/2023/24/46-percent-more-solar-energy-production-in-2022) (IEA PVPS Task 1. https://iea-pvps.org/wp-content/uploads/2023/10/National-Survey-Report-of-PV-Power-Applications-in-SWITZERLAND-September-2023-v01-1.pdf). Furthermore, Norway and Sweden are not included and their PV production data is generally unavailable, however these issues can be resolved by calculating the yearly power generation with the installed solar capacity (which is far more readily available for each country) and global horizontal irradiance (GHI) for each country or state, which is commonly called [26] the "main PV resource".

The GHI information for each country or state can be found on Global Solar Atlas (World Bank Group & Solargis. https://globalsolaratlas.info/) wherein the average of the maximum and minimum is taken. Then, to estimate the power production, this average is multiplied by the number of days in a year along with an efficiency factor (typically given as 0.75) (IEA PVPS Methodology Guidelines on Life Cycle Assessment of Photovoltaic Electricity. https://iea-pvps.org/wp-content/uploads/2020/01/rep12_11.pdf) and with the solar capacity. In the case of Europe, the final used solar power production, which we denominate P, is an average between the reported and estimated solar power production in TWh, and because of the previously mentioned ENTSO-E bias, the estimated production is typically slightly lower than the real production. In the case of USA and Canada, P is the yearly data obtained through above mentioned sources. In most cases, sources for 2022 have been used since 2023 data would have been biased by the emissions themselves, and in the rare cases where this was not possible, 2021 data was used instead. The sources (papers, publications, official reports etc.) for the capacities used in the final calculation of P are displayed in Table 1.

Table 1: PV capacity sources used in P calculation for Europe.

Regions	PV Capacity Source
Germany, Italy, Netherlands	Bocca et. al. (2015) [60]
UK, Norway, Belgium, Switzerland, Denmark	Renewable Energy Capacity Statistics 2022. The International Renewable Energy Agency (IRENA). https://www.irena.org/-/media/Files/IRENA/Agency/Publication/2022/Apr/IRENA_RE_Capacity_Statistics_2022.pdf
Sweden	"Sweden deployed 1 GW of PV in 2022". pv magazine International. https://www.pv-magazine.com/2023/01/25/sweden-deployed-1-gw-of-pv-in-2022/
Austria	"Austria deployed more than 1.4 GW of new solar in 2022." pv magazine International. https://www.pv-magazine.com/2023/01/09/austria-deployed-more-than-1-4-gw-of-new-solar-in-2022/
Croatia	"Croatia has 776 MW in 25,406 solar power plants connected to distribution grid." Balkan Green Energy News. https://balkangreenenergynews.com/croatia-has-776-mw-in-25406-solar-power-plants-connected-to-distribution-grid/
Czech Republic	"Czech Republic adds 970MWp solar PV plants to grid in 2023." PV Tech. https://www.pv-tech.org/czech-republic-adds-970mwp-solar-pv-plants-to-grid-in-2023/
France	National Survey Report of PV Power Applications in France 2023. IEA Photovoltaic Power Systems Programme (IEA PVPS). https://iea-pvps.org/wp-content/uploads/2024/10/Fact-Sheet-NSR-France-1.pdf
Spain	National Survey Report of PV Power Applications in Spain 2022. IEA Photovoltaic Power Systems Programme (IEA PVPS). https://iea-pvps.org/wp-content/uploads/2023/08/National-Survey-Report-of-PV-Power-Applications-in-Spain-2022.pdf

Portugal	“Wind and solar produce more than half of Portugal’s electricity for the first time.” Ember. https://ember-energy.org/latest-updates/wind-and-solar-produce-more-than-half-of-portugals-electricity-for-the-first-time/
Slovenia	“Slovenian Solar Photovoltaic (PV) Power Market with Stellar Growth in 2022 and Excellent Development Opportunities by 2030.” Renewable Market Watch. https://renewablemarketwatch.com/news-analysis/slovenian-solar-photovoltaic-pv-power-market-with-stellar-growth-in-2022-and-excellent-development-opportunities-by-2030/
Hungary	“Hungary's solar capacity surged by 1.6 GW in 2023 to 5.6 GW.” Enerdata. https://www.enerdata.net/publications/daily-energy-news/hungarys-solar-capacity-surged-16-gw-2023-56-gw.html
Romania	“Romania Installed 624 MW New Electricity Capacity in 2023.” TaiyangNews. https://taiyangnews.info/markets/romania-installed-624-mw-new-electricity-capacity-in-2023
Bulgaria	“Bulgaria Solar Photovoltaic (PV) Power Market: Outlook 2023–2032.” Renewable Market Watch. https://ineaconsulting.eu/en/news-en/bulgaria-solar-photovoltaic-pv-power-market-outlook-2023-2032-by-renewable-market-watch-with-trends-forecasts-investments-opportunities-analysis
Greece	“Greece Targets 34.5 GW Total PV Capacity By 2050.” TaiyangNews. https://taiyangnews.info/markets/greece-targets-34-5-gw-total-pv-capacity-by-2050
Poland	Photovoltaic Market in Poland 2025. EC BREC Institute for Renewable Energy (IEO). https://ieo.pl/en/
Slovakia	Slovak Renewable Electricity Market Report 2022. Slovak Association of Photovoltaic Industry and RES (SAPI). https://www.sapi.sk/files/Slovak-Renewable-Electricity-Market-Report-2022.pdf
Lithuania	Renewable Energy Capacity Statistics 2023. International Renewable Energy Agency (IRENA). https://www.developmentaid.org/api/frontend/cms/file/2023/03/IRENA_RE_Capacity_Statistics_2023.pdf
Estonia	“Developing 40 MW of Solar PV in Estonia.” Black & Veatch. https://www.bv.com/projects/developing-40-mw-of-solar-pv-in-estonia

All these above-mentioned issues contribute to dissuading us from fully committing to monthly data, even though in some cases this data is available. For Canada and Europe, official monthly data can be obtained through the national statistical office of Canada (Statistics Canada. https://www150.statcan.gc.ca/t1/tbl1/en/cv.action?pid=2510001501) and through previously mentioned ENTSO-E resources, even though in the case of ENTSO-E, monthly data for some countries does not exist and as mentioned before, is not fully quantitatively reliable. However, for the USA, this data only seems to exist through the Ember repository (Ember. https://ember-energy.org/data/us-electricity-data/). Monthly Ember data, by comparison with official data from our regions of interest, can generally be deemed not reliable enough from a quantitative perspective due to provisional reporting, behind-the-meter solar discrepancies, and data being provided on an “as is” basis (Ember. https://ember-energy.org/latest-insights/european-electricity-review-2025/supporting-materials/).

After establishing yearly solar power production data (P) for each analysed country and state, it is possible to determine the 5-monthly solar power production. To estimate this fraction, monthly production from ENTSO-E and Ember is used as previously mentioned and it is compared to the final used solar power production like so:

$$P_{5-monthly} = P\frac{p_{May}+p_{June}+p_{July}+p_{August}+p_{September}}{p_{year}} = P \cdot SR \quad (4)$$

wherein p_{year} is the sum of the monthly solar power data in the monthly ENTSO-E and Ember repositories for each country or state, p_{May} through $p_{September}$ represents the monthly data itself. In this manner, the obtained fraction is quantitatively correct since the datasets are used in a qualitative manner to derive a percentage of the corrected yearly production. For European countries which are not included in the ENTSO-E monthly dataset, we have used a generic solar monthly distribution template that has the approximated percentage of yearly production for each month of a typical upper mid-latitude European country. This is, in essence, an approximate SR, and it is not extracted from a single source but is consistent with publicly available datasets, some of which have already been mentioned either for capacity or production. Thus, we take the percentages for May-September as 12%, 13%, 14%, 14%, 11%, therefore the 5-monthly production for these analysed countries or states is:

$$P_{5-monthly} = \frac{12+13+14+14+11}{100} P = 0.64P \tag{5}$$

In both cases, the modelled production difference due to aerosols will follow as:

$$\Delta P_{5-monthly} = P_{5-monthly} \frac{\Delta R}{100} = SR \cdot P \frac{R_{FIRE} - R_{noFIRE}}{R_{noFIRE}} \tag{6}$$

The form of this equation shall be maintained throughout this work, thus not taking into consideration the mechanical specifications of all PV installations in the affected regions. This is a reasonable approximation to make, given that most (circa 98%) of the commercially employed solar panels are constructed from crystalline silicon and the rest from cadmium telluride (IEIA-PVSP Trends in Photovoltaic Applications 2025. https://iea-pvps.org/wp-content/uploads/2025/10/IEA-PVPS_Trends_2025-.pdf). A precise consideration of the importance of various types of hardware in the FIRE-noFIRE impacts falls beyond the scope of this paper. To proceed with obtaining the modelled $\Delta P_{5-monthly}$, the model surface downwelling shortwave flux data for each state and country is obtained using their latitude and longitude boundaries obtained using the Nominatim geocoding service (OpenStreetMap Foundation. https://nominatim.openstreetmap.org/ui/search.html) on the ΔR map as shown in Fig. 3 and averaging over those boundaries. For any further consideration, the supplementary material contains a table describing the reported PV capacity, estimated yearly production, reported yearly production, 5-monthly production, modelled production difference due to wildfire aerosols and percentage modelled production difference due to aerosols for each country or state analysed in our work (Table 1-S).

The 5-monthly PV energy deficit will necessarily lead to a carbon footprint, since the deficit will need to be supplemented by other sources of electric energy. To calculate this carbon burden, the lost energy is converted to MWh and then multiplied by a marginal emission factor (typically in tons of CO_2 /MWh), which yields how many tons of CO_2 the given country or state had to emit via alternative energy sources in order to supplement the PV energy loss. The equation is:

$$F_{CO_2} = 1000 \cdot \Delta P^{total}_{5-monthly} \cdot EF_m \tag{7}$$

Factor data sources are listed in Table 2.

Table 2: Marginal emission factor sources.

Regions	Marginal Emission Factor Source
Most of Europe	Bastos, Joana; Monforti-Ferrario, Fabio; Melica, Giulia (2024): GHG Emission Factors for Electricity Consumption. European Commission, Joint Research Centre (JRC). https://data.jrc.ec.europa.eu/dataset/919df040-0252-4e4e-ad82-c054896e1641
USA	eGRID 2022 Summary Tables. U.S. Environmental Protection Agency (EPA). https://www.epa.gov/system/files/documents/2024-01/egrid2022_summary_tables.pdf
Canada	"Emission Factors and Reference Values." Government of Canada. https://www.canada.ca/en/environment-climate-change/services/climate-change/pricing-pollution-how-it-will-work/output-based-pricing-system/federal-greenhouse-gas-offset-system/emission-factors-reference-values.html
Switzerland	Romano et. al. (2024) [61]

Finally, it is also possible to estimate monetary losses due to PV production deficit for each country or state, by obtaining market electricity price data (kWh, all taxes included), and by multiplying this data with the modelled production loss. Sources for these electricity prices can be found in Table 3.

Table 3: Market electricity price sources.

Regions	Market Electricity Price Source
Most of Europe	Electricity Prices for Non-Household Consumers – Annual Data (NRG_PC_204). Eurostat. https://ec.europa.eu/eurostat/databrowser/view/nrg_pc_204__custom_17702395/default/table
UK	"Average Cost of Electricity per kWh in the UK (2025)." NimbleFins. https://www.nimblefins.co.uk/average-cost-electricity-kwh-uk
USA	"Retail Electricity Prices: Understanding Trends and Implications." Most Policy Initiative. https://mostpolicyinitiative.org/science-note/retail-electricity-prices/
Switzerland	"ElCom Forecasts a 27% Increase for Electricity Prices in Switzerland in 2023." Enerdata. https://www.enerdata.net/publications/daily-energy-news/elcom-forecasts-27-increase-electricity-prices-switzerland-2023.html

The cost calculation arises from a market-based approach as an approximation, since more advanced methods of calculating these costs, such as a marginal replacement cost calculation approach coupled with a consideration of contractual and subsidy costs, are outside the scope of this paper. However, a secondary consideration can be added to the emission cost, referring to the social cost of carbon attached to the previously calculated CO_2 burden. It is known that establishing regional social carbon costs is a difficult task, however a recent study [62] finds a reasonable estimate for this cost at $185 per ton in 2022. This means that the extra estimated total social carbon cost across all countries and states is 379.13 million euros, which has been added to the modelled total monetary deficit. Other potential cost calculations could include the market cost of carbon credits, however the average price of one credit was approximately $7.37 in 2023 (Ecosystem Marketplace. https://www.ecosystemmarketplace.com/publications/state-of-the-voluntary-carbon-market-report-2023/), thus the added cost is quite small compared to the total. Regarding marginal replacement generation, PV marginal cost is often close to zero since PV production has very low operational marginal cost and zero fuel cost, meaning that, if PV production is diminished and is then replaced by other sources, then the system often does incur approximately the market value of the missing electricity, meaning that our market-based approximation is likely very close to the real monetary loss.

Acknowledgements

We acknowledge the assistance of prof. Ioannis Kountouris of the Centre for Environmental Policy and Leverhulme Centre for Wildfires, Imperial College London, who aided us in shaping the financial segment of the wildfire impact analysis contained in this work. This work was supported by computational time granted from the National Infrastructures for Research and Technology S.A. (GRNET S.A.) in the National HPC facility - ARIS - under project ID FirePC (pr017) and FirePC2 (pr018).

Funding Declaration

This work was funded through the Hellenic Foundation for Research and Innovation (Grant no. 3453), and with the assistance of the AXA Research Fund (project "AXA Chair in Wildfires and Climate", CPO00163217) and of the Leverhulme Trust (grant no. RC-2018-023) through the Leverhulme Centre for Wildfires, Environment and Society. Further support for this research was obtained through the project "Support the upgrading of the operation of the National Network on Climate Change (CLIMPACT)" of the General Secretariat of Research and Technology (grant no. 2023NA11900001), and from the Horizon Europe programme under Grant Agreement No. 101137680 via project CERTAINTY (Cloud-aERosol inTeractions & their impActs IN The earth sYstem).

Data Availability

All model data generated during this study are publicly available at 10.5281/zenodo.18963011. CMIP6 SSP370 data used to initialize the model as per the specified configuration used in our experiments can be found at https://doi.org/10.22033/ESGF/CMIP6.4885. CAMS GFAS 2023 wildfire emission data are available at https://doi.org/10.24381/a05253c7. Additionally, this study uses Himawari data downloaded from the Data Integration and Analysis System (DIAS) by Japan Agency for Marine-Earth Science and Technology (JAMSTEC). ERA5 precipitation and zonal wind data can be found at https://doi.org/10.24381/cds.f17050d7.

Code Availability

The code associated with this study is publicly available at 10.5281/zenodo.18963011. The EC-Earth3 code is available from the EC-Earth development portal for members of the consortium. Permission to access the EC-Earth3 source code can be requested from the EC-Earth community via the EC-Earth website (http://www.ec-earth.org/) and may be granted if a corresponding software license agreement is signed with ECMWF.

Author Contributions

I.A.R. developed the initial hypothesis, produced the model runs, wrote most of the code associated with the research, wrote the main manuscript text, produced the figures. M.W.J originated the initial hypothesis, assisted with conceptual advice and manuscript redaction advice, assisted in developing conclusions of results. M.G. provided manuscript redaction advice, assisted in the improvement and production of the figures, assisted in data analysis, helped with the code associated with the research. M.P.P. provided manuscript redaction advice, assisted in the improvement and production of the figures, assisted in data analysis. M.K. provided conceptual advice and model expertise, provided manuscript redaction advice, analysed the figures. R.N.M. assisted with the technical aspect of the model runs, assisted the production of the model runs, facilitated the organization of the involved model datasets and methods. L.G. assisted with identifying, compiling and contributing to the analysis of official solar power production data. A.V. supervised the research, provided conceptual advice and model expertise, provided manuscript redaction advice, analysed the figures, validated the research conclusions. All authors have read and approved the manuscript. All authors reviewed the manuscript and contributed significantly to the finalization of this research.

Competing Interests

The authors declare that they have no competing interests as defined by Nature Portfolio, or other interests that might be perceived to influence the results and/or discussion reported in this paper.

References

[1] Haegel, N. M., Margolis, R., Buonassisi, T., Feldman, D., Froitzheim, A., Garabedian, R., ... & Kurtz, S. (2017). Terawatt-scale photovoltaics: Trajectories and challenges. Science, 356(6334), 141-143.

[2] Solangi, K. H., Islam, M. R., Saidur, R., Rahim, N. A., & Fayaz, H. (2011). A review on global solar energy policy. Renewable and sustainable energy reviews, 15(4), 2149-2163.

[3] Feldman, D., Ramasamy, V., Fu, R., Ramdas, A., Desai, J., & Margolis, R. (2021). US solar photovoltaic system and energy storage cost benchmark: Q1 2020 (pp. 1-120). Golden, CO: National Renewable Energy Laboratory.

[4] Wendisch, M., & Yang, P. (2012). Theory of atmospheric radiative transfer: a comprehensive introduction. John Wiley & Sons.

[5] Wallace, J. M., & Hobbs, P. V. (2006). Atmospheric science: an introductory survey (Vol. 92). Elsevier.

[6] Boucher, O. (2015). Atmospheric aerosols. Atmospheric Aerosols: Properties and Climate Impacts (pp. 9-24). Dordrecht: Springer Netherlands.

[7] Kaufman, Y. J., Tanré, D., & Boucher, O. (2002). A satellite view of aerosols in the climate system. Nature, 419(6903), 215-223.

[8] Hess, M., Koepke, P., & Schult, I. (1998). Optical properties of aerosols and clouds: The software package OPAC. Bulletin of the American meteorological society, 79(5), 831-844.

[9] Li, X., Mauzerall, D. L., & Bergin, M. H. (2020). Global reduction of solar power generation efficiency due to aerosols and panel soiling. Nature Sustainability, 3(9), 720-727.

[10] Neher I., Buchmann T., Crewell S., Pospichal B. & Meilinger S. (2019). Impact of atmospheric aerosols on solar power. Meteorologische Zeitschrift (Contributions to Atmospheric Sciences), Meteorologische Zeitschrift, 4, 28.

[11] Hirsch, E., & Koren, I. (2021). Record-breaking aerosol levels explained by smoke injection into the stratosphere. Science, 371(6535), 1269-1274.

[12] Pyne, S. J. (1984). Introduction to wildland fire. Fire management in the United States (pp. xix+-455).

[13] Johnson, E. A., & Johnson, E. A. (1996). Fire and vegetation dynamics: studies from the North American boreal forest. Cambridge University Press.

[14] Mangeon, S. et al. INFERNO: A fire and emissions scheme for the UK Met Office's Unified Model. Geo-Sci. Model Dev. 9, 2685–2700 (2016).

[15] Westerling, A. L., Hidalgo, H. G., Cayan, D. R., & Swetnam, T. W. (2006). Warming and earlier spring increase western US forest wildfire activity. Science, 313(5789), 940-943.

[16] Abatzoglou, J. T., & Williams, A. P. (2016). Impact of anthropogenic climate change on wildfire across western US forests. Proceedings of the National Academy of sciences, 113(42), 11770-11775.

[17] McClure, C. D., & Jaffe, D. A. (2018). US particulate matter air quality improves except in wildfire-prone areas. Proceedings of the National Academy of Sciences, 115(31), 7901-7906.

[18] O'Dell, K., Ford, B., Fischer, E. V., & Pierce, J. R. (2019). Contribution of wildland-fire smoke to US PM2. 5 and its influence on recent trends. Environmental science & technology, 53(4), 1797-1804.

[19] Ford, B., Val Martin, M., Zelasky, S. E., Fischer, E. V., Anenberg, S. C., Heald, C. L., & Pierce, J. R. (2018). Future fire impacts on smoke concentrations, visibility, and health in the contiguous United States. GeoHealth, 2(8), 229-247.

[20] Knorr, W., Dentener, F., Lamarque, J. F., Jiang, L., & Arneth, A. (2017). Wildfire air pollution hazard during the 21st century. Atmospheric Chemistry and Physics, 17(14), 9223-9236.

[21] Sun, K., Lu, L., Jiang, Y., Wang, Y., Zhou, K., & He, Z. (2018). Integrated effects of PM2. 5 deposition, module surface conditions and nanocoatings on solar PV surface glass transmittance. Renewable and Sustainable Energy Reviews, 82, 4107-4120.

[22] Gómez-Amo, J. L., Freile-Aranda, M. D., Camarasa, J., Estellés, V., Utrillas, M. P., & Martínez-Lozano, J. A. (2019). Empirical estimates of the radiative impact of an unusually extreme dust and wildfire episode on the performance of a photovoltaic plant in Western Mediterranean. Applied Energy, 235, 1226-1234.

[23] Perry, M., & Troccoli, A. (2015). Impact of a fire burn on solar irradiance and PV power. Solar Energy, 114, 167-173.

[24] Gilletly, S. D., Jackson, N. D., & Staid, A. (2023). Evaluating the impact of wildfire smoke on solar photovoltaic production. Applied Energy, 348, 121303.

[25] Donaldson, D. L., Piper, D. M., & Jayaweera, D. (2021). Temporal solar photovoltaic generation capacity reduction from wildfire smoke. IEEE Access, 9, 79841-79852.

[26] Corwin, K. A., Burkhardt, J., Corr, C. A., Stackhouse Jr, P. W., Munshi, A., & Fischer, E. V. (2025). Solar energy resource availability under extreme and historical wildfire smoke conditions. Nature Communications, 16(1), 245.

[27] Jain, P., Barber, Q. E., Taylor, S. W., Whitman, E., Castellanos Acuna, D., Boulanger, Y., ... & Parisien, M. A. (2024). Drivers and impacts of the record-breaking 2023 wildfire season in Canada. Nature Communications, 15(1), 6764.

[28] Byrne, B., Liu, J., Bowman, K. W., Pascolini-Campbell, M., Chatterjee, A., Pandey, S., ... & Sinha, S. (2024). Carbon emissions from the 2023 Canadian wildfires. Nature, 633(8031), 835-839.

[29] MacCarthy, J., Tyukavina, A., Weisse, M. J., Harris, N., & Glen, E. (2024). Extreme wildfires in Canada and their contribution to global loss in tree cover and carbon emissions in 2023. Global Change Biology, 30(6), e17392.

[30] Stocker, M., Ladstädter, F., & Steiner, A. K. (2021). Observing the climate impact of large wildfires on stratospheric temperature. Scientific reports, 11(1), 22994.

[31] Peterson, D. A., Campbell, J. R., Hyer, E. J., Fromm, M. D., Kablick III, G. P., Cossuth, J. H., & DeLand, M. T. (2018). Wildfire-driven thunderstorms cause a volcano-like stratospheric injection of smoke. NPJ climate and atmospheric science, 1(1), 30.

[32] Chen, H., Zhang, W. & Sheng, L. Canadian record-breaking wildfires in 2023 and their impact on US air quality. Atmos. Environ. 342, 120941 (2025).

[33] Roșu, I. A., Mourgela, R. N., Kasoar, M., Boleti, E., Parrington, M., & Voulgarakis, A. (2025). Large-scale impacts of the 2023 Canadian wildfires on the Northern Hemisphere atmosphere. npj Clean Air, 1(1), 22.

[34] Döscher, R., Acosta, M., Alessandri, A., Anthoni, P., Arneth, A., Arsouze, T., ... & Zhang, Q. (2021). The EC-earth3 Earth system model for the climate model intercomparison project 6. Geoscientific Model Development Discussions, 2021, 1-90.

[35] Kaiser, J. W. et al. Biomass burning emissions estimated with a global fire assimilation system based on observed fire radiative power. Biogeosciences 9, 527–554 (2012).

[36] D'alessandro, W., Giammanco, S., Parello, F., & Valenza, M. (1997). CO2 output and δ13C (CO2) from Mount Etna as indicators of degassing of shallow asthenosphere. *Bulletin of Volcanology*, *58*(6), 455-458.

[37] Voulgarakis, A., & Field, R. D. (2015). Fire influences on atmospheric composition, air quality and climate. Current Pollution Reports, 1(2), 70-81.

[38] Black, C., Tesfaigzi, Y., Bassein, J. A., & Miller, L. A. (2017). Wildfire smoke exposure and human health: Significant gaps in research for a growing public health issue. Environmental toxicology and pharmacology, 55, 186-195.

[39] Wang, D., Guan, D., Zhu, S., Kinnon, M. M., Geng, G., Zhang, Q., ... & Davis, S. J. (2021). Economic footprint of California wildfires in 2018. Nature Sustainability, 4(3), 252-260.

[40] Reid, C. E., Brauer, M., Johnston, F. H., Jerrett, M., Balmes, J. R., & Elliott, C. T. (2016). Critical review of health impacts of wildfire smoke exposure. Environmental health perspectives, 124(9), 1334-1343.

[41] Mahdavi, A., Farhadi, M., Gorji-Bandpy, M., & Mahmoudi, A. (2022). A review of passive cooling of photovoltaic devices. Cleaner Engineering and Technology, 11, 100579.

[42] Nakamoto, Y., & Eguchi, S. (2024). How do seasonal and technical factors affect generation efficiency of photovoltaic power plants?. Renewable and Sustainable Energy Reviews, 199, 114441.

[43] Breeze, P. (2016). Chapter 10: Modules, inverters, and solar photovoltaic systems. In Solar power generation. Academic Press.

[44] Yuan, J., Blaabjerg, F., Yang, Y., Sangwongwanich, A., & Shen, Y. (2019). An overview of photovoltaic microinverters: Topology, efficiency, and reliability. In 2019 IEEE 13th International Conference on Compatibility, Power Electronics and Power Engineering (CPE-POWERENG) (pp. 1-6). IEEE Press.

[45] Panagea, I. S., Tsanis, I. K., & Koutroulis, A. G. (2017). Climate change impact on photovoltaic energy output: the case of Greece. In Climate Change and the Future of Sustainability (pp. 85-106). Apple Academic Press.

[46] Russo, M. A., Carvalho, D., Martins, N., & Monteiro, A. (2023). Future perspectives for wind and solar electricity production under high-resolution climate change scenarios. Journal of Cleaner Production, 404, 136997.

[47] van Noije, T., Bergman, T., Le Sager, P., O'Donnell, D., Makkonen, R., Gonçalves-Ageitos, M., ... & Yang, S. EC-Earth3-AerChem, a global climate model with interactive aerosols and atmospheric chemistry participating in CMIP6. Geoscientific Model Development Discussions, 1-46 (2020).

[48] van Gerrevink, M. J., Veraverbeke, S., Cooperdock, S., Potter, S., Zhong, Q., Moubarak, M., ... & Rogers, B. M. (2026). Climate impacts from North American boreal forest fires. Nature Geoscience, 1-7.

[49] Liu, Y., Zhang, K., Qian, Y., Wang, Y., Zou, Y., Song, Y., ... & Yang, X. Q. (2018). Investigation of short-term effective radiative forcing of fire aerosols over North America using nudged hindcast ensembles. Atmospheric Chemistry and Physics, 18(1), 31-47.

[50] Yoshioka, M., Regayre, L. A., Pringle, K. J., Johnson, J. S., Mann, G. W., Partridge, D. G., ... & Carslaw, K. S. (2019). Ensembles of global climate model variants designed for the quantification and constraint of uncertainty in aerosols and their radiative forcing. Journal of Advances in Modeling Earth Systems, 11(11), 3728-3754.

[51] Zhong, Q., Schutgens, N., Van Der Werf, G., Van Noije, T., Tsigaridis, K., Bauer, S. E., ... & Myhre, G. (2022). Satellite-based evaluation of AeroCom model bias in biomass burning regions. Atmospheric Chemistry and Physics Discussions, 2022, 1-47.

[52] Koffi, B., Schulz, M., Bréon, F. M., Dentener, F., Steensen, B. M., Griesfeller, J., ... & Zhang, K. (2016). Evaluation of the aerosol vertical distribution in global aerosol models through comparison against CALIOP measurements: AeroCom phase II results. Journal of Geophysical Research: Atmospheres, 121(12), 7254-7283.

[53] Fountoulakis, I., Papachristopoulou, K., Proestakis, E., Amiridis, V., Kontoes, C., & Kazadzis, S. (2022). Effect of aerosol vertical distribution on the modeling of solar radiation. Remote Sensing, 14(5), 1143.

[54] Mishra, A. K., Koren, I., & Rudich, Y. (2015). Effect of aerosol vertical distribution on aerosol-radiation interaction: A theoretical prospect. Heliyon, 1(2).

[55] Neher, I., Buchmann, T., Crewell, S., Evers-Dietze, B., Pfeilsticker, K., Pospichal, B., ... & Meilinger, S. (2017). Impact of atmospheric aerosols on photovoltaic energy production Scenario for the Sahel zone. Energy Procedia, 125, 170-179.

[56] Ishaque, K., Salam, Z., & Taheri, H. (2011). Simple, fast and accurate two-diode model for photovoltaic modules. Solar energy materials and solar cells, 95(2), 586-594.

[57] Skoplaki, E., & Palyvos, J. A. (2009). On the temperature dependence of photovoltaic module electrical performance: A review of efficiency/power correlations. Solar energy, 83(5), 614-624.

[58] Notton, G., Cristofari, C., Mattei, M., & Poggi, P. (2005). Modelling of a double-glass photovoltaic module using finite differences. Applied thermal engineering, 25(17-18), 2854-2877.

[59] Evans, D. L. (1981). Simplified method for predicting photovoltaic array output. Solar energy, 27(6), 555-560.

[60] Bocca, A., Chiavazzo, E., Macii, A., & Asinari, P. (2015). Solar energy potential assessment: An overview and a fast modeling approach with application to Italy. Renewable and Sustainable Energy Reviews, 49, 291-296.

[61] Romano, E., Patel, M. K., & Hollmuller, P. (2024). Applying trade mechanisms to quantify dynamic GHG emissions of electricity consumption in an open economy-The case of Switzerland. Energy, 311, 133398.

[62] Rennert, K., Errickson, F., Prest, B. C., Rennels, L., Newell, R. G., Pizer, W., ... & Anthoff, D. (2022). Comprehensive evidence implies a higher social cost of CO2. Nature, 610(7933), 687-692.

Figure Captions

Figure 1: Regional May-September 2023 modelled (FIRE – noFIRE) impacts: a) NA PV production difference ($\Delta P_{5-monthly}^{total}$), b) NA CO_2 burden (F_{CO_2}), c) NA monetary deficit, d) Europe PV production difference ($\Delta P_{5-monthly}^{total}$), e) Europe CO_2 burden (F_{CO_2}), f) Europe monetary deficit. More information on data sources in “Solar power production data sources and processing”

subsection of the "Methods" section. Primary Python packages used for plotting include "matplotlib", "cartopy" and "geopandas".

Figure 2: Regional 2023 EF_m and SR analysis: a) NA, and b) Europe. More information on data sources in "Solar power production data sources and processing" subsection of the "Methods" section. Primary Python packages used for plotting include "matplotlib", "cartopy" and "geopandas".

Figure. 3: Northern Hemisphere May-September 2023 modelled average differences (FIRE – noFIRE) for: a) surface downwelling shortwave flux, b) surface temperature.